Contributed paper

OPTO-ELECTRONICS REVIEW **14**(2), 149–154

One dimensional model of dye-doped nematic layer for holography

G. DERFEL*[1], M. BUCZKOWSKA[1], and J. PARKA[2]

[1]Institute of Physics, Technical University of Łódź, 219 Wólczańska Str., 93-005 Łódź, Poland
[2]Institute of Applied Physics, Military University of Technology, 2 Kaliskiego Str., 00-908 Warsaw, Poland

The layer of electrically conducting nematic liquid crystal doped with photosensitive dye and confined between polyimide coated electrodes can serve as a diffraction grating. In this paper, the deformations of the nematic director field induced in such a system by external voltage were studied numerically by means of one-dimensional model. The dissociation and recombination of ions were taken into account according to weak electrolyte model. The director orientation in the deformed layers and the distributions of the electric field and of the ion concentrations were calculated for blocking and for conducting electrodes. The effective extraordinary refractive index was also determined as a function of average ion concentration.

Keywords: holographic gratings, photoinduced director reorientation, electric field distribution, director field, deformations of dye-doped nematic layer.

1. Introduction

Nematic liquid crystals offer an interesting possibility of applications in the field of optical data processing [1]. Due to their unique dielectric, elastic, and optical properties, the effective refractive indices of a nematic layer can be modulated by controlled changes of director alignment. Such modulation enables us to form holographic gratings. Several systems have been considered in which the photoinduced director reorientation can be realized. The torque leading to the director reorientation can be caused by optical field [2], electric field [3] or by intermolecular interactions [4]. Here, we focus our attention on the director reorientation induced by incident light in the nematic material which is doped with suitable photosensitive dye [5–9].

Several processes can be distinguished in the observed effects [5]. The possible scenarios which are taken into account involve charge generation, ion transport, charge separation, electric field formation and director field distortion.

Let us consider a nematic liquid crystal layer doped with a photosensitive dye and homogenously aligned by polyimide films deposited on transparent electrodes. Such a system can serve as a diffraction grating. Its principle of operation can be briefly described as follows [7,8]. The light interference pattern is projected on the layer. The dc voltage U, higher than the threshold voltage for Freedericksz transition U_c, is applied between the electrodes. The director field within the liquid crystal is distorted by the electric field due to the voltage drop U_{LC} across the nematic layer. The U_{LC} value depends on the relative magnitudes of the resistivity of the liquid crystal and that of the polymer coating. The former is influenced by external illumination of the layer surface. In the non illuminated regions of the system, the liquid crystal specific resistivity is higher than in the illuminated areas. The corresponding voltage drop exceeds significantly the threshold, $U_{LC} >> U_c$, which gives rise to strong deformation of the director field. On the contrary, in the illuminated regions, the resistivity of the nematic is decreased because of photogeneration of ions, which is due to the presence of the photoexcitable dopant. The U_{LC} value is therefore reduced and the director field deformation is weaker. In consequence, various parts of the layer illuminated with different intensity differ in their effective refractive indices n_e^{eff}. Such a system can therefore work as a phase diffraction grating and can be applied for optically addressed real time holography devices.

One of the possible mechanisms of charge carriers photogeneration assumes formation of heterolytic complexes resulting from interaction between excited dye molecules and liquid crystal molecules [9]. The number of complexes is proportional to the light intensity. The proportionality constant depends on the dye concentration and on these properties of the dye molecule that decide about its interaction with light wave. The complexes may dissociate into ions, therefore the number of ions is also proportional to the intensity of illumination. The quantitative details of the relation between the ion concentration and the light intensity remain unknown.

In this paper, we present numerical analysis of one dimensional model of a nematic liquid crystal layer doped with a photosensitive dye. We did not consider the details of the photogeneration of the ions. In our calculations, we used the average ion concentration instead of the light intensity, basing on the assumption of the proportionality between these both quantities. Therefore we attributed the

*e-mail: gderfel@p.lodz.pl

high concentration values to bright regions of the layer and the low values to dark regions. The polyimide films were treated as simple ohmic resistors. The calculations concerned the nearly planar nematic layer with finite surface anchoring strength. Our aim was to find the director orientation profiles and spatial distribution of the electric field and of the ionic space charges for various ion contents corresponding to various incident light intensities. In order to characterise the optical properties of the nematic layer we have also calculated its effective extraordinary refractive index. The electric current across the layer was taken into account. For this purpose, we adopted a simplified model of electrical phenomena occurring at the boundaries of the nematic layer as well as the weak electrolyte model of the nematic in the bulk.

2. Method

2.1. Geometry and parameters

The infinite nematic liquid crystal layer of the thickness $d = 6.3$ μm, parallel to the xy plane of the Cartesian co-ordinate system and positioned between $z = -d/2$ and $z = d/2$ was considered. The nematic layer was confined between two electrodes coated with 0.1 μm thick polyimide films. The nearly planar alignment with the surface tilt angle $\theta_s = 1°$ was assumed. The anchoring strength W was identical on both surfaces and was equal to 2×10^{-5} J/m^2. The director **n** was parallel to the xz plane. Its orientation was defined by the angle $\theta(z)$, measured between **n** and the x axis. The model substance was characterised by the elastic constants $k_{11} = 7.5\times10^{-12}$ N and $k_{33} = 9.5\times10^{-12}$ N. The positive dielectric anisotropy of the nematic was adopted with the dielectric constant components $\varepsilon_{\parallel} = 12$ and $\varepsilon_{\perp} = 4$. The refractive indices were $n_{\perp} = 1.521$ and $n_{\parallel} = 1.674$. These parameters were chosen according to the properties of the liquid crystal 6CHBT (4-trans-4'-n-hexyl-cyclohexyl-isothiocyanatobenzene) [10]. The average ion concentration N_{av}, defined as

$$N_{av} = \frac{1}{2d}\left\{\int_{-d/2}^{d/2}[N^+(z) + N^-(z)]dz\right\}, \tag{1}$$

where $N^{\pm}(z)$ denotes the concentrations of ions of a corresponding sign, ranged from 10^{18} to about 3×10^{20} m^{-3}. The calculations were performed for two values of voltage applied between the electrodes, $U = 8$ V and $U = 12$ V. These values belong to the range of voltages for which the maximum diffraction is typically observed in the cells with a thickness of a few micrometers. The lower ($z = -d/2$) electrode was earthed. The voltages across the liquid crystal layer, U_{LC}, were always greater than the threshold $U_c = 1.023$ V. The polyimide coatings with specific resistivity $r = 10^{10}$ Ω m were considered as ohmic resistors.

The transport of the ions in the liquid crystal was characterised by their mobility and diffusion coefficients. It was assumed that the mobility of the positive ions was much smaller than that of the negative ions [11]. Their values used in calculations corresponded to typical results of mobility measurements in various liquid crystals and reflected typical anisotropy of mobility $\mu_{\parallel}^- = 1.5\times10^{-9}$ m^2/Vs, $\mu_{\perp}^- = 1\times10^{-9}$ m^2/Vs, $\mu_{\parallel}^+ = 1.5\times10^{-10}$ m^2/Vs, and $\mu_{\perp}^+ = 1\times10^{-10}$ m^2/Vs [12,13]. The Einstein relation was assumed for the diffusion constants $D_{\parallel,\perp}^{\pm} = (k_B T/q)\mu_{\parallel,\perp}^{\pm}$ where q is the absolute value of the ionic charge, k_B is the Boltzmann constant and T is the absolute temperature $T = 300$ K. The weak electrolyte model [14] was adopted in which the ion concentration was determined by the generation and recombination constants. The generation constant β depended on the electric field strength E according to the Onsager theory [15,16],

$$\beta = \beta_0\left(1 + \frac{q^3}{8\pi\varepsilon_0\bar{\varepsilon}k_B^2T^2}E\right),$$

where $\bar{\varepsilon} = (2\varepsilon_{\perp} + \varepsilon_{\parallel})/3$. In the absence of the field, its value β_0 was varied in the range 10^{20}–10^{24} m^{-3}s^{-1} in order to control the ion concentration. The recombination constant α was equal to 3.5×10^{-18} m^{3}s^{-1}. It was calculated from Langevin theory [15], $\alpha = 2q\bar{\mu}/\varepsilon_0\bar{\varepsilon}$, where the average mobility was expressed by

$$\bar{\mu} = [(2\mu_{\perp}^+ + \mu_{\parallel}^+)/3 + (2\mu_{\perp}^- + \mu_{\parallel}^-)/3]/2.$$

3. Basic equations

The problem is considered to be one-dimensional. The reduced co-ordinate, $\zeta = z/d$, is introduced in the following. The functions $\theta(\zeta)$ and $V(\zeta)$ which describe the director orientation and the potential distribution within the layer respectively are determined by the torque equation

$$\frac{1}{2}(k_b - 1)\sin 2\theta\left(\frac{d\theta}{d\zeta}\right)^2 + (\cos^2\theta + k_b\sin^2\theta)\frac{d^2\theta}{d\zeta^2}, \tag{2}$$
$$+\frac{1}{2}\frac{\varepsilon_0\Delta\varepsilon}{k_{11}}\sin 2\theta\left(\frac{dV}{d\zeta}\right)^2 = 0$$

and the electrostatic equation

$$\rho(\zeta)d^2 + \varepsilon_0(\varepsilon_{\perp} + \Delta\varepsilon\sin^2\theta)\frac{\partial^2 V}{\partial\zeta^2}, \tag{3}$$
$$+\varepsilon_0\Delta\varepsilon\sin 2\theta\frac{\partial V}{\partial\zeta}\frac{\partial\theta}{\partial\zeta} = 0$$

where $k_b = k_{33}/k_{11}$ and $\rho(\zeta) = q[N^+(\zeta) - N^-(\zeta)]$ is the space charge density.

The transport of ions in the bulk is governed by two equations of continuity of the ion fluxes

$$d(\beta - \alpha N^+N^-) = \frac{dJ_z^{\pm}}{d\zeta}, \tag{4}$$

where

$$J_z^{\pm} = \mp\frac{1}{d}\left(\mu_{zz}^{\pm}N^{\pm}\frac{dV}{d\zeta} \pm D_{zz}^{\pm}\frac{dN^{\pm}}{d\zeta}\right)$$

denotes the flux of ions of the given sign, i.e., the number of ions which pass through a surface ζ = const, counted per unit area and per unit time. The z-components of mobility and diffusion coefficients are given by $\mu_{zz}^{\pm} = \mu_{\perp}^{\pm} + \Delta\mu^{\pm} \sin^2\theta$ and $D_{zz}^{\pm} = D_{\perp}^{\pm} + \Delta D^{\pm} \sin^2\theta$, respectively, where $\Delta\mu^{\pm} = \mu_{\parallel}^{\pm} - \mu_{\perp}^{\pm}$ and $\Delta D^{\pm} = D_{\parallel}^{\pm} - D_{\perp}^{\pm}$ denote the anisotropies of both quantities.

The boundary conditions for $\theta(\zeta)$ are determined by the equations

$$\pm\left[\cos^2(\pm 1/2) + k_b \sin^2\theta(\pm 1/2)\right]\left.\frac{d\theta}{d\zeta}\right|_{\pm 1/2} + \frac{1}{2}\gamma \sin 2\left[\theta(\pm 1/2) - \theta_s\right] = 0 \qquad (5)$$

for $\zeta = \pm 1/2$, where $\gamma = Wd/k_{11}$. The boundary conditions for the potential are $V(-1/2) = 0$ and $V(1/2) = U_{LC}$.

In order to establish the boundary conditions for the ion concentrations in the nematic, a suitable model is necessary. As the electrodes are coated with the aligning layers, we assumed that the ions are generated and discharged at the interface between the liquid crystal and polyimide. The equilibrium state at the electrodes is described by four equations. Each equation expresses the fact that the number of ions of the given sign approaching a chosen electrode (or moving away from it) per unit area and per unit time is equal to the net change in the number of ions which results from the generation and neutralisation processes at the electrode. The speed of neutralisation of the ions, $n_r^{\pm}$, is proportional to their concentration: $n_r^{\pm} = K_r^{\pm} N^{\pm}$ and the speed of generation, $n_g^{\pm}$, is proportional to the concentration N_d of the neutral dissociable molecules: $n_g^{\pm} = K_g^{\pm} N_d$, where $K_r^{\pm}$ and $K_g^{\pm}$ are suitable constants of proportionality. In the case of zero applied voltage, the equilibrium state realises in which $N^{\pm} = N_0 = \sqrt{\beta_0/\alpha}$. Therefore $K_r^{\pm} N_0 = K_g^{\pm} N_d$. Since $N^{\pm} << N_d$, one can neglect any changes of N_d. This enables us to determine $K_g^{\pm}$ if $K_r^{\pm}$ and N_d are estimated. In general, $K_g^{\pm}$ and $K_r^{\pm}$ may be different for each electrode process. For simplicity however, we performed the calculations using common value of K_r for all neutralisation processes as well as common value of $K_g = K_r N_0/N_d$ for all generation processes at the electrodes.

The rates of generation and neutralisation of the ions at the electrodes can be interpreted in terms of a model in which they are determined by the activation energies φ of corresponding electrochemical reactions. For instance, the rate of neutralisation of the negative ion occurring by the transfer of an electron from the ion to the electrode is expressed by $K_r = k_r \exp(-\varphi/k_B T)$, where k_r is a constant. Similar formula can be used for the generation rate constant of positive ions occurring by the transfer of an electron from a neutral molecule to the electrode. In general, the energy barriers φ can be of different height for every electrode process. The energy barrier is affected by the electric field existing at the electrode, i.e., increased or decreased by $\Delta\varphi = EqL$, where L is the thickness of double layer in which the ions are discharged or generated. It is of the order of several molecular lengths. In our calculations L = 10 nm.

As a result of the above assumptions, the boundary conditions take a form

$$\mp\mu_{zz}^{\pm} N^{\pm}\frac{dV}{d\zeta} - D^{\pm}\frac{dN^{\pm}}{d\zeta} = [-N^{\pm}K_r \exp(\pm\Delta\varphi/k_B T) + N_0 K_r \exp(\mp\Delta\varphi/k_B T)]d \quad \text{for } \zeta = -1/2 \qquad (6)$$

$$\mp\mu_{zz}^{\pm} N^{\pm}\frac{dV}{d\zeta} - D^{\pm}\frac{dN^{\pm}}{d\zeta} = [-N^{\pm}K_r \exp(\mp\Delta\varphi/k_B T) + N_0 K_r \exp(\pm\Delta\varphi/k_B T)]d \quad \text{for } \zeta = +1/2 \qquad (7)$$

The left-hand sides of these equations represent the fluxes of the ions at the electrodes. The first terms on the right-hand sides denote the numbers of ions which are neutralised and the second terms – the numbers of ions generated at the electrodes in the course of accepting or donating the electron by the neutral molecule.

The calculations were carried out with two values of K_r: 10^{-6} m/s and 10^{-3} m/s, which corresponded to the blocking and conducting electrodes respectively, whereas N_d was equal to 10^{24} m^{-3} in every case.

The set of ten equations given by Eqs. (2–7) was solved numerically. The director configurations [described by the angle $\theta(\zeta)$], the electric potential distributions $V(\zeta)$ and the ion concentrations $N^{\pm}(\zeta)$ were calculated for various generation constants β_0 which gave different voltage drops U_{LC} which in turn caused distinct deformations of the director field. The consequences of deformations for the optical properties of the layer were illustrated by the effective extraordinary index defined as

$$n_e^{eff} = \int_{-1/2}^{1/2} \frac{n_{\perp} n_{\parallel}}{\sqrt{[n_{\parallel}\sin\theta(\zeta)]^2 + [n_{\perp}\cos\theta(\zeta)]^2}} d\zeta. \qquad (8)$$

4. Results

The calculations were performed for two external voltages, U = 8 V and U = 12 V, and for two values of K_r, 10^{-6} m/s and 10^{-3} m/s, which corresponded to the blocking and conducting electrodes respectively.

4.1. Director distribution

There is no sharp threshold voltage for the deformation of the nematic layer due to the non-zero surface tilt angle. Nevertheless, remarkable distortions may arise only if the U_{LC} voltage exceeds some value which is close to U_c. The most interesting phenomena occur if $U_{LC} >> U_c$, i.e., when the director is aligned nearly perpendicular to the plane of the layer in prevailing part of its thickness. The structure of the layer is described by the director orientation angle $\theta(\zeta)$.

The functions $\theta(\zeta)$ calculated for several U_{LC} voltages are shown in Fig. 1 for U = 12 V. In the case of blocking electrodes, the director profiles are asymmetric [Fig. 1(a)], i.e., the deformations are stronger in the negative half of the layer. For conducting electrodes [Fig. 1(b)], a slight asymmetry is visible at moderate voltages, e.g., at U_{LC} = 2 V. One can also notice that in the case of the blocking electrodes the deformations develop less rapidly with increasing U_{LC}. Identical results were obtained for U = 8 V if only the U_{LC} values were the same.

4.2. Electric field distribution

Large non-uniform electric fields, reaching 2×10^6 V/m, arise in the vicinity of the boundaries, as shown for U = 12 V in Fig. 2. These fields are stronger in the case of blocking electrodes [Fig. 2(a)] than in the case of conducting electrodes [Fig. 2(b)]. The $E(\zeta)$ distributions for blocking electrodes are asymmetric, especially at higher U_{LC}. In the case of conducting electrodes, the asymmetry is very weak [Fig. 2(b)]. The distributions $E(\zeta)$ obtained for U = 8 V are practically the same. In all the cases, the electric field strength in the bulk is lower than U_{LC}/d.

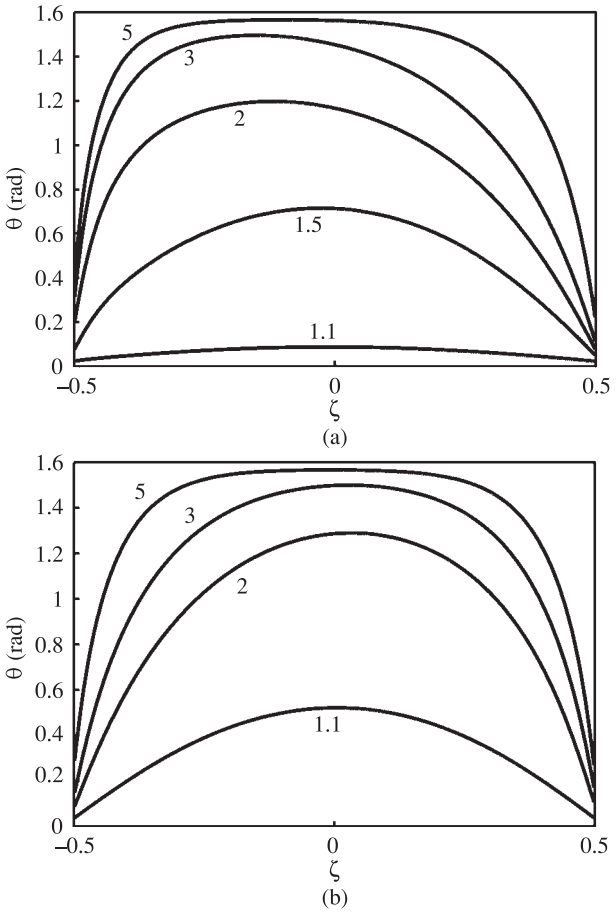

Fig. 1. Director distributions illustrated by $\theta(\zeta)$ functions at U = 12 V, (a) blocking electrodes and (b) conducting electrodes; the U_{LC} values (in volts) are indicated at each curve.

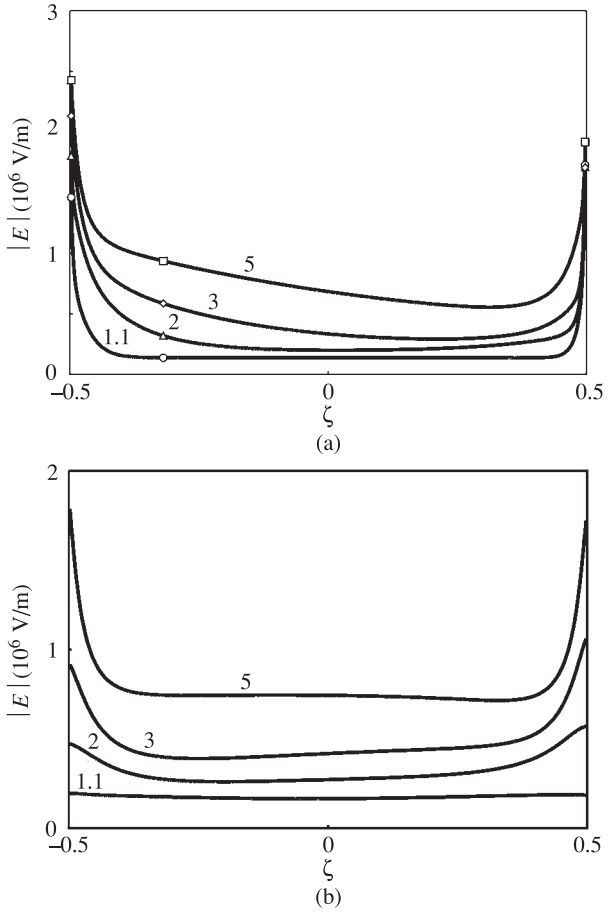

Fig. 2. Electric field strength in the layer $E(\zeta)$ at U = 12 V, (a) blocking electrodes, (squares, triangles and circles allow to identify the values of $|E(\pm1/2)|$), (b) conducting electrodes. The U_{LC} values (in volts) are indicated at each curve.

4.3. Ions distribution

The total number of positive ions per unit area of the layer differs from the number of the negative ions. It means that under the action of the external voltage, the layer becomes electrically non-neutral. In the case of blocking electrodes, the ions are accumulated at the opposite electrodes. Their concentrations in the bulk are negligible in comparison with the subelectrode charges. There is an excess of positive ions in this case. The distributions for the case of conducting electrodes are shown in Fig. 3 for U = 12 V. The sign of the excess ions depends on U_{LC}. The $N^{\pm}(\zeta)$ distributions obtained for U = 8 V are qualitatively the same.

4.4. Effective extraordinary refractive index

The optical properties of the layer that are essential for applications in holography can be characterised by the effective extraordinary refractive index defined by Eq. (8). It may adopt values ranging from $n_{\perp}$ = 1.521 to $n_{\parallel}$ = 1.672, for ideally homeotropic and undeformed layer respectively. The value of n_e^{eff} is determined by the director distribution

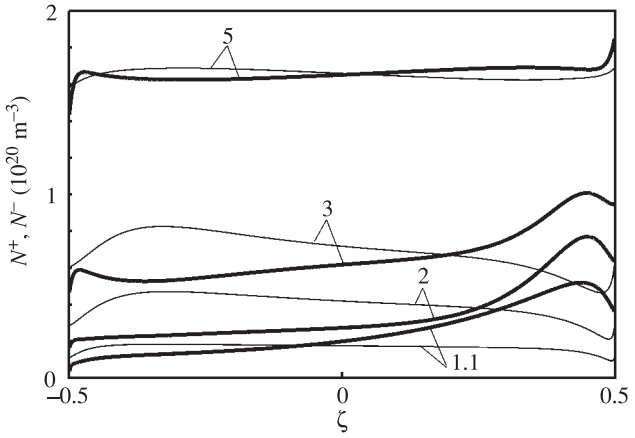

Fig. 3. Distributions of positive ions (thick lines) and negative ions (thin lines) in the case of conducting electrodes, U = 12 V, the U_{LC} values (in volts) are indicated at each curve.

in the deformed layer. It depends on the voltage drop U_{LC}, which in turn is a consequence of the resistivity of the layer resulting from the concentration of the ions. The dependencies of n_e^{eff} on the average ion concentration are shown in Fig. 4. In order to vary the n_e^{eff} index over the entire possible range, the change of the average ion concentration by nearly an order of magnitude is required. The corresponding range of the ion concentration depends on K_r and U. In the case of conducting electrodes, the values of N_{av} which affect the effective index belong to the range 10^{19}–10^{20} m^{-3} at U = 8 V and to the range 2×10^{19}–2×10^{20} m^{-3} at U = 12 V. The concentrations which give the same effect for blocking electrodes are several times higher but they cover somewhat narrower range. Since one may assume that for some range of intensity of the incident light the average ion concentration increases with the intensity, the presented results suggest that the brighter illumination is required in the case of higher external voltages and blocking electrodes than in the opposite case.

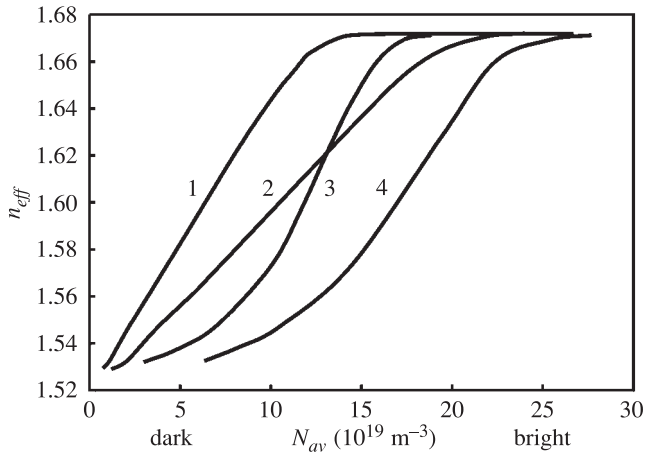

Fig. 4. Effective extraordinary refractive index n_e^{eff} as a function of the average ion concentration N_{av}, curve 1 – U = 8 V, $K_r = 10^{-3}$ m/s, curve 2 – U = 12 V, $K_r = 10^{-3}$ m/s, curve 3 – U = 8 V, $K_r = 10^{-6}$ m/s, and curve 4 – U = 12 V, $K_r = 10^{-6}$ m/s.

5. Discussion

In this paper, we consider the deformations of the nematic liquid crystal layer induced by dc voltage and light illumination. The liquid crystal layer is placed between polyimide coated ITO electrodes with blocking or conducting contacts and contains ions of various concentrations. Such system can serve as a simplified one-dimensional model of the processes taking place in the liquid crystal cell with holographic grating pattern. In the case of this kind of grating, the bright regions are in close neighbourhood of the dark regions. The deformations in the neighbouring regions are different and interact one upon another. The ion concentrations in these areas are also different and give rise to the transverse electric field as well as to the ionic current. Obviously, the two-dimensional approach would be more adequate for the description of the grating. Nevertheless, one may suppose that the functions $\theta(\zeta)$), $E(\zeta)$, and $N^{\pm}(\zeta)$ found for the one-dimensional case are satisfactory approximation of the analogous functions of the two-dimensional system. Theoretical studies of certain two-dimensional models are reported in Refs. 5 and 17, however, the electric field distribution, as well as the ion concentration distributions were assumed to be sinusoidally varying with the z and x co-ordinates, thus neglecting the effects of ions separation in external field.

The liquid crystal layer subjected to the external voltage becomes asymmetric. The asymmetry is manifested in the director field deformations, in the distributions of the electric field and of the ions and also in different contents of the positive and negative ions, which makes the whole layer electrically non-neutral. The only reason for those effects is the difference in the mobilities of the positive and negative ions and, in consequence, in their diffusion coefficients.

While the accumulation of the ions at the blocking electrodes of opposite signs seems to be reasonable, the ions distributions in the case of $K_r = 10^{-3}$ m/s is less intuitive. These effects result from the complex equilibrium between generation and neutralisation of ions at the electrodes and the dissociation and neutralisation influenced by the electric field in the vicinity of them. The screening effect due to the ions manifests itself by the less rapid dependence of the deformations on the U_{LC} voltage in the blocking case.

The dependence of n_e^{eff} on the average ion concentration in the case of blocking electrodes is somewhat stronger in some ranges of N_{av} than in the case of $K_r = 10^{-3}$ m/s. This may suggest that the n_e^{eff} is more sensitive to variations of illumination in the case of blocking boundary conditions, which may result in better diffraction efficiency than in the opposite case.

The presented results reveal that in the case of conducting nematic the properties of the electrode contacts affect the deformation of the liquid crystal and therefore influence the optical properties of the layer.

References

1. I.C. Khoo, *Liquid Crystals Physical Properties and Nonlinear Optical Phenomena*, Wiley, New York, 1995.
2. I. Marrucci and Y.R. Shen, "Nonlinear optics of liquid crystals", in *The Optics of Thermotropic Liquid Crystals*, Chapter 6, p. 115, edited by S. Elston and R. Sambles, Taylor & Francis, London, 1998.
3. L.M. Blinov and V.G. Chigrinov, *Electro-optic Effects in Liquid Crystal Materials*, Springer Verlag, New York, 1993.
4. I. Janossy and A.D. Lloyd, "Low-power reorientation in dyed nematics", *Mol. Cryst. Liq. Cryst.* **203**, 77 (1991).
5. I.C. Khoo, "Optical dc-field induced space charge fields and photorefractive-like holographic grating formation in nematic liquid crystals", *Mol. Cryst. Liq. Cryst.* **282**, 53–66 (1996).
6. E.V. Rudenko and A.V. Sukhov, "Optically induced spatial charge separation in nematic and the resultant orientational nonlinearity", JETP **78**, 875–882 (1994).
7. S. Bartkiewicz and A. Miniewicz, "Mechanism of optical recording in doped liquid crystals", *Adv. Mater. Opt. Electron.* 6, 219–224 (1996).
8. A. Miniewicz, J. Parka, S. Bartkiewicz, and A. Januszko, "Liquid crystals as materials for real time holographic optical device", *Pure Appl. Opt.* **7**, 179–189 (1998).
9. A. Miniewicz, S. Bartkiewicz, A. Januszko, and J. Parka, "Dye-doped liquid crystal composite for real-time holography: nematic reorientation induced by photoconductivity", in *Photoactive Organic Materials Science and Application*, NATO ASI Series, Vol. 3/9, pp. 487–496, edited by F. Kajzar, V.M. Agranovich, and C.Y.C. Lee, Kluwer Academic, Dordrecht, 1996.
10. J. Parka, A. Miniewicz, A. Januszko, Y. Reznikov, R. Dąbrowski, and Z. Stolarz, "Influence of nematic liquid crystal with dye and cell construction parameters on dynamic holographic grating formation", *Proc. SPIE* **4147**, 335–339 (2000).
11. H. Naito, M. Okuda, and A. Sugimura, "Transient discharging processes in nematic liquid crystals", *Phys. Rev.* **A44**, R3434–R3437 (1991).
12. S. Naemura, Y. Nakazono, K. Nishikawa, A. Sawada, P. Kirsch, M. Bremer, and K. Tarumi, "Structure of ions in liquid-crystalline materials", *Mat. Res. Soc. Symp. Proc.* **508**, 235–240 (1998).
13. G. Derfel and A. Lipiński, "Charge carrier mobility measurements in nematic liquid crystals", *Mol. Cryst. Liq. Cryst.* **55**, 89–99 (1979).
14. G. Briere, F. Gaspard, and R. Herino, "Cinetique de dissociation et relaxation de conduction ionique en phase liquide", *J. Chim. Phys.* **68**, 845 (1971).
15. H. de Vleeschouwer, A. Verschueren, F. Bougriona, R. Van Asselt, E. Alexander, S. Vermael, K. Neyts, and H. Pauwels, "Long-term ion transport in nematic liquid crystal displays", *Jpn. J. Appl. Phys.* **40**, 3272–3276 (2001).
16. L. Onsager, "Deviations from Ohm's law in weak electrolytes", *J. Chem. Phys.* **2**, 599–615 (1934).
17. G. Zhang, G. Montemezzani, and P. Günter, "Orientational photorefractive effect in nematic liquid crystal with externally applied fields", *J. Appl. Phys.* **88**, 1709–1717 (2000).

